Accepted Manuscript

Experimental study on fatigue performance of adhesively bonded anchorage system for CFRP tendons

Gui-hua Xie, Yong-sheng Tang, C.M. Wang, Shi-quan Li, Rong-gui Liu

PII: S1359-8368(18)30751-0

DOI: 10.1016/j.compositesb.2018.05.047

Reference: JCOMB 5717

To appear in: *Composites Part B*

Received Date: 7 March 2018

Revised Date: 19 May 2018

Accepted Date: 27 May 2018

Please cite this article as: Xie G-h, Tang Y-s, Wang CM, Li S-q, Liu R-g, Experimental study on fatigue performance of adhesively bonded anchorage system for CFRP tendons, *Composites Part B* (2018), doi: 10.1016/j.compositesb.2018.05.047.

Experimental Study on Fatigue Performance of Adhesively Bonded Anchorage System for CFRP Tendons

Gui-hua XIE[1,2*], Yong-sheng TANG[1], C. M. WANG[2], Shi-quan LI[1,3], Rong-gui LIU[1]
[1]Faculty of Civil Engineering and Mechanics, Jiangsu University,
Zhenjiang 212013, China
[2]School of Civil Engineering, The University of Queensland, St Lucia,
Queensland 4072, Australia
[3]College of Urban Construction and Design, Taizhou Institute of Science and Technology,
Taizhou 225309, China
*Corresponding author's e-mail address: guihua.xie@uq.edu.au

Abstract: This study is concerned with the fatigue performance of adhesively bonded anchorage for carbon fiber reinforced polymer (CFRP) tendons subjected to cyclic loading. Series of monotonous and cyclic experiments under different stress amplitudes and loading frequencies were carried out in order to investigate the mechanical performance of bonded anchorage systems for CFRP tendons and to study the influence of cyclic loading on the anchoring performance. The fatigue damage and the relationships between damage, loading frequency and interfacial temperature rise of anchorage systems were analyzed. The results show that cyclic tension-tension loading is instrumental in enhancing the synergistic interaction between the anchorage components and it also stabilizes the entire anchorage system performance provided that the stress amplitude is kept lower than 10% of the ultimate tensile capacity of the anchorage systems and the maximum stress is less than 50% of the ultimate capacity of the anchorage system. The loading frequency influences significantly the temperature variation in the anchorage system. A high loading frequency may result in a sharp temperature rise at the early-stage and mid-stage of cyclic tension-tension loading, followed by a rather stable late stage. This phenomenon of temperature rise during fatigue tests may indicate the extent of fatigue damage in the anchorage system.

Keywords: Carbon Fiber Reinforced Polymer; Anchorage system; Fatigue; Slippage; Temperature rise; Damage

1 Introduction

Cable stayed bridges and suspension bridges are beautiful structures with excellent spanning capacity. There have been considerable advancement in long-span bridge technology with the development of materials. For example, the materials for cables have developed from degradable vegetable fibers in ancient times to modern ultra-high tensile strength (2000 MPa) steel cables [1]. The availability of such high-strength steel makes possible the construction of long-cable stayed bridges with spans greater than 1000 m, such as the Russky Bridge in Russia with a span of 1104m, and Sutong Yangtze River Bridge in China with a span of 1088m. In the case of suspension bridges, the spans are even longer. For example, the Akashi-Kaikyo bridge in Japan has a free span of 1991m. The load-carrying efficiency and spanning ability of long-span bridges are also restricted by the heavy deadweight of the structures. Bridge engineers have to develop very stiff, strong and lightweight deck structures by using new composite materials with a high strength-to-weight ratio for greater bridge spans.

Bridge engineers have to also contend with structural corrosion problems and fatigue that have been major causes of many catastrophic failures of bridges. According to the final report from the U.S. Department of Commerce Census Bureau in 2002, the annual direct cost for maintenance and repair against corrosion damage for national highway bridges is estimated to be between $6.43 billion and $10.15 billion with an average annual cost of corrosion amounting to $8.29 billion. Indirect costs due to traffic delays and lost productivity were estimated at more than ten times the direct cost of corrosion maintenance, repair and rehabilitation [2]. Therefore, corrosion protection of bridge structures is expensive and poses challenges to bridge engineers to this day. Moreover, steel elements are commonly used in bridge structures and they are also expected to be vulnerable to fatigue and fracture. For example, the railway bridge over the Skellefte River in Sweden suffered fatigue cracking at the threaded part of the hanger due to a combination of oscillations and secondary bending of the hangers at their connections to the steel arch. Fatigue cracking also occurs in various bridge elements with coped ends or cut-short flanges at their connections to other elements [3]. A report from the federal highway administration of the US Department of Transportation stated that about 40% of metallic highway bridges in the USA in 2005 have deteriorated significantly as a result of cyclic vehicular loads [4]. Thus, improvement of bridge resistance to corrosion and fatigue is vital for the integrity and durability of bridge structures.

An interesting new material that has been introduced for bridge engineering is the Carbon Fibre Reinforced Polymer (CFRP). The first CFRP cable structure in the world is the Tsukuba FRP bridge in 1996 [5]. Comprising high-performance thermosetting resin and high-strength fibres, CFRP has special characteristics in the mechanical and in-service characteristics such as high resistance to fatigue, lightweight, anticorrosion, high tensile strength and stiffness [5, 6]. This combination of properties makes CFRP an attractive alternative to steel for cables in large-scale cable stayed bridges. Hitherto, a large amount of research studies on the design methodology and performance of long-span cable stayed bridges with CFRP cables

have been carried out. Xie *et al.* [7] investigated the effect of the geometric nonlinearity of CFRP cables on static and dynamic properties of cable-stayed bridges by carrying out tests on the bridge at site as well as performing numerical simulations. They found that the long-span bridge with CFRP cables has a higher resistance against wind-induced vibration than its counterpart with steel cables. Yang *et al.* [8] studied the vibration characteristics of CFRP and Basalt Fibre-Reinforced Polymer (BFRP) cables in long-span cable stayed bridges by determining the in-plane and out-of-plane vibrations of reduced-scale bridge models. They discovered that the risk of cable-deck resonance was lower than that of bridges with steel cables and the equivalent damping properties of in-plane and out-of-plane vibrations revealed significant difference when compared to steel cables. Cai *et al.* [9] used genetic algorithms to optimize the combination of CFRP and traditional steel material for the hybrid cable system with the aim of improving the aerodynamic performance of long-span cable stayed bridges.

Although great progress has been achieved in the design methodology and performance of long-span bridges with CFRP cables, there are still challenges hindering the wide applications of CFRP cables in prestressed bridges. One of these challenges is the difficulty in anchoring the prestressed CFRP tendons because they are vulnerable to damage or premature failure under transverse loads at the anchorage area. This is because the CFRP tendon is brittle and highly anisotropic (since its transverse strength is only about one twentieth of its longitudinal strength). Therefore, the traditional methods for anchoring steel bars or strands cannot be applied for CFRP tendons directly. Numerous efforts from researchers [e.g. 10-19] came up with three basic types of anchorage systems for CFRP tendons with respect to load transfer mechanism, namely, (1) adhesively bonded anchorage system (such as in Fig. 1a), (2) mechanical clamping anchorage system (such as in Fig. 1b) and (3) composite bonding- wedge anchorage system (such as in Fig. 1c).

The adhesively bonding anchorage system consists of a sleeve and bonding medium, usually epoxy resin, cement grout or high-performance concrete, with or without an inner cone in the sleeve. In this anchorage system, CFRP tendons are anchored via chemical bonding provided by bonding medium, and mechanical interlocking and friction at the bonding medium/CFRP tendon interface which is determined by the inner sleeve surface coarseness, the inner inclination of the sleeve and the material properties. The anchorage performance and shear distribution in the anchoring zone play a crucial role in taking full advantage of high tensile strength of CFRP tendons. This anchorage system has attracted the attention of many researchers. Puigvert *et al.* [13] conducted experimental static tests of different shapes and sizes of anchorage, and performed numerical simulations for different adhesive material models with the view to investigate the static response of the adhesively bonded anchorage and its failure mechanism. They found that the cohesive zone model with progressive damage was the most reasonable for describing and predicting the approximate distribution of shear stress in the epoxy bonded anchorages among the other models. Feng *et al.* [15] characterized the mechanical properties of single-rod and a multi-rod straight- pipe bonded anchorage by using the finite element method.

They found that the straight-parabolic inner cone has a clear effect on reducing the shear force at the loading end, and the design parameters such as the modulus and thickness of the adhesive, inner inclined angle, and the space between the rods significantly influence the anchoring performance. Fang *et al*. [17] performed experiments on multi-rod anchorages and formulated the bond strength and critical bond length for CFRP rods embedded in an ultra-high performance Reactive Powder Concrete. Meier *et al.* [18, 20] proposed the Gradient Anchorage System in anchoring the two CFRP cables of the Stork Bridge located in Winterthur, Switzerland. They changed the elastic modulus of the resin along with the axis of the bonded anchorage to lower the peak of shear stress in the anchoring zone and hence improved the anchorage efficiency. Research studies continue to seek the optimal shear stress distribution and further improvement of anchoring efficiency.

The second type of anchorage system for single CFRP tendon is the mechanical clamping anchorage system comprising wedges, anchoring ring and soft metal tube, shown in Fig. 1b. This kind of anchorage relies mainly on the friction at the interface between the tendon and the inner surface of wedges, as well as the perpendicular grasping force to provide the anchoring force. The application of the soft metal tube is to protect the CFRP tendon from damage caused by the "teeth" in the wedges as large forces are transferred to the tendon. Even so, the CFRP tendon held by this anchorage system is susceptible to premature failure resulting from the high shear stresses arising from the gripping action at the leading edge of the wedges. Especially, the experimental results indicate that the difference between a successful anchorage and an unsuccessful anchorage is small, that is, the stability of this kind of anchorage is unreliable [19]. Details of the kind of anchorage have been given in [12, 19, 21-23].

The third type of anchorage system is the composite wedge-bonding anchorage system as shown in Fig. 1c. This anchorage system utilizes the advantages of adhesively bonded anchorages and mechanical clamping anchorages for providing a higher anchoring force by combining the roles of bonding material and gripping function. Thus, its performance and ultimate tensile capacity is highly sensitive to the combined methods, material properties and the geometrical characteristics of the anchorage system. Details of these anchorages have been discussed in [11,16].

The influence of repeated or cyclic loading on anchoring performance adds another dimension to the difficulty in anchoring CFRP tendons. Bridges are often exposed to millions of traffic load cycles during their service life, which may lead to fatigue damage. Investigations by Haghani *et al*. [3] have shown that fatigue damage was the main cause in many bridge failures. Cracks may be formed during the course of the fatigue damage accumulation and eventually propagate through the material, resulting in either a local or a total failure of the bridge structure. Thus, structural members of bridges should not only be designed for static load capacity, but also have to meet the requirements in dynamic performances, such as fatigue and cyclic loadings. There has been considerable interest in the fatigue behaviour of reinforced concrete beams and bridge girders strengthened or retrofitted by FRP laminates. The crucial factors and the significant influence on fatigue performance have been investigated in detail in these references [24-27]. Also, the fatigue failure criteria for

crack initiation in metallic beams reinforced by external bonding CFRP plates were discussed [28]. Martinelli et al. [29, 30] have studied the theoretical bond-slip model for the adhesive interface of FRP-to-concrete adhesive joints under loading/unloading cycling tests. As for anchorages for FRP tendons, Elrefai *et al.* [22] carried out an experimental study to investigate the fatigue performance of a wedge anchorage for CFRP tendons under different cyclic loading stress ranges from 10% to 17% of the ultimate strength of the tendon with two minimum stress levels of 40% and 47% of the ultimate strength. They concluded that the fatigue life of the wedge anchorage was primarily affected by the applied stress range, and the minimum stress could hardly influence the fatigue life. Puigvert *et al.* [31] conducted experimental and numerical studies on epoxy adhesively bonded anchorages. They stated that the fatigue life had a better correlation with the maximum fatigue load than the loading range, and the anchorages with thicker adhesive layers had a longer fatigue life under the same fatigue load. However, the anchorages with thinner adhesive thickness had a longer fatigue life at the same normalized fatigue load with respect to the static ultimate load. Zhuge *et al.* [32] found that most part of the relative displacement between the anchorage assemblies of wedge-type anchorages during the fatigue tests was generated mainly by the maximum tensile load before cyclic loading, and the displacement had no effect on the mechanical properties of anchorage system. However, it has yet to be confirmed whether these conclusions are applicable for bonded-type anchorages.

So far, there is relatively little research on fatigue performance of anchorage systems for CFRP tendons. The limited research studies focused mainly on checking whether the anchorage system for FRP tendons (specially designed by the researchers) could pass through the preset fatigue tests. Little attention was paid to the damage features and the influences of loading frequency and temperature on the internal damage of anchorage systems under fatigue loading. This makes the investigation on fatigue mechanism and the nature of damage propagation of anchorage systems for FRP tendons even more urgent; before seeking an optimal design of anchorage system for application in bridges. The present work, therefore, will focus on the static and fatigue performances of the adhesively bonded anchorage for single-CFRP tendon with the view to uncover the fatigue mechanism and damage characteristics of the bonded-type anchorages, as well as to explore the relationship between the loading frequency, temperature rise and cumulative damage of the anchorage systems under fatigue loading. This study adopts the adhesively bonded anchorage system because it has the advantage of reducing the transverse load to the tendons in order to minimize damage to the tendons.

The layout of this paper is as follows. In Section 2, the materials, specimen preparation and methods are presented for the static and fatigue tests on adhesively bonded anchorage systems. In Section 3, the results from the static and fatigue tests are reported. In Section 4, the analysis on the static performance of anchorage systems before and after fatigue tests are presented, followed by the discussion on fatigue damage mechanism and temperature effect. Section 5 presents the main conclusions of this study.

2 Materials and Methods

The static and fatigue tests were carried out with the aim to investigate the fatigue performance and damage mechanism of resin-based bonded anchorage for CFRP tendons. The anchorage system consists of the bonding material, metal sleeve with an inner inclination and a CFRP tendon which was held in place by the bonding material along the axis of the sleeve as shown in Fig. 2.

2.1Materials and specimens

Unidirectional 8mm-diameter CFRP tendons were utilized for the static and fatigue experiments. The contents of fibre and resin in CFRP tendons were 65% and 35% by volume, respectively. The tendons have equally spaced shallow notches on their surfaces. Their mechanical properties in longitudinal and transverse directions are listed in Table 1 where UTS denotes the ultimate tensile strength.

The sleeve was made from a high-quality structural steel with the carbon content of 0.45% and the surface roughening treatment method was applied for the inner wall of the sleeve. The minimum gap between the tendon and the inner wall of sleeve was 8mm which equals the diameter of the tendon.

The two different bonding materials used were:

- *Adhesive Ⅰ* - a Lica-300A/B adhesive produced by Nanjing Hi-tech Composites Co., Ltd, China. Components A and B were mixed evenly and poured into the sleeve directly by a special glue gun.
- *Adhesive Ⅱ* - a kind of resin mortar specially manufactured before the tests. This resin mortar is Lica-300A/B adhesive reinforced by adding quartz sand. The diameter of quartz sand particles used in the tests fell in two categories that depends on the size, i.e., 0.5mm to 1mm diameter sand particle for one category and 1mm to 1.5mm diameter sand particle for the second category. The adopted mass ratio of the finer sand category to the coarser sand category is 2:1. The epoxy resin and sand that made up Adhesive Ⅱ were proportioned by a mass ratio of 2:1. The average compressive strength of the Adhesive Ⅱ was tested to be 68MPa.

An anchorage specimen to be filled with Adhesive Ⅱ was manufactured in accordance to the following steps:

- Step 1: Quartz sand of 80g with the particle diameters ranging from 0.5mm to 1mm and another kind of quartz sand of 40g with the diameters ranging from 1mm to 1.5mm were mixed evenly.
- Step 2: Lica-300 A/B adhesive was squeezed out and mixed by a glue gun. When the color of the mixed adhesive became uniform, the adhesive of 240g was mixed with the prepared quartz sand mixture until the new homogeneous mixture was made.
- Step 3: The new mixture was fully poured into a steel sleeve which was closed at one end by a plug, accompanied by slight vibration of the anchorage so as to avoid the formation of air bubbles and to improve the compaction of the bonding material.

- Step 4: The CFRP tendon was potted along the axis of the sleeve accurately. The excessive grout was wiped off and the other end of the sleeve was closed by a copper sheet.
- Step 5: The anchorage was put in a shelf vertically. The anchorage was fully cured for a minimum of three days. Then another anchorage was manufactured for the other end of the CFRP tendon by the same method.
- Step 6: The specimens were cured under the room temperature for at least three weeks.

2.2 Experimental Methods

2.2.1 Static Tensile Experiments

Previous experimental results reveal that small differences in the mounting procedure and design parameters of anchorages may significantly influence the performance of anchorages. Thus, a group of adhesively bonded anchorages for CFRP tendons was taken for axial tensile tests with the view to obtain the static performance and the average tensile capacity. The anchorage system with the highest tensile capacity was then selected to carry out the following tensile-tensile fatigue tests with a constant stress amplitude. Specimens' information for static tests is listed in Table 2.

The static tests were carried out according to the *Technical Specification for Application of Anchorage, Grip and Coupler for Prestressing Tendons (J1006-2010)* [33]. All static tests were carried out in the Material Testing System (MTS 809). The experimental setup is shown in Fig. 3. The tensile load was applied in steps of 10% of the nominal tensile capacity F_{t0} of the tendon with a loading rate of 100MPa/min. When the load reached 70% of F_{t0}, the load was kept for 20 minutes and thereafter the load was increased again until the specimen failed.

2.2.2 Fatigue Experiments

The fatigue performance of the specimens under cyclic tension-tension loading was investigated by using two different experimental devices, *viz.* MTS-809 and PA-500 (see Fig. 3) in order to mitigate the risk caused by the precision of the loading device. According to the provisions given by the *Technical Code for FRP Composites in Construction GB50608* and *ACI 440*, structural members have to pass through the 2 million-cycle fatigue tests with the maximal stress of 50% of the tensile strength of CFRP tendons and the stress amplitude of at least 80MPa, and fatigue failure should not occur during fatigue loading. This acceptable criterion for CFRP tendon anchorage system has been adopted for this study. Referring to this criterion, the pertinent details of the fatigue loading are listed in Table 3. Loading ceases when one of the following conditions was reached:

- Large slippage occurs in the anchorage zone and the system can no longer resist loads efficiently;
- CFRP tendon cracks or fractures;
- Serious debonding failure appears at the interface between the adhesive and

sleeve or at the adhesive/tendon interface;

- Load cycle count reaches the maximum repeated time preset for fatigue tests.

The maximum number of cycles is set to be 2 million for all fatigue tests. In order to save on experimental time and cost, the tests are terminated when system slippage varies marginal in the last loading stage and no important damage can be observed (which indicates the anchorage system begins to be stable under fatigue loading).

All specimens were subjected to a small monotonous static tension before fatigue loading so as to stabilize the anchorage system. The static preloading value was set to be 30kN in order to avoid any damage caused by the monotonous pre-tensioning process. A sinusoidal fatigue loading was applied for Specimens P-1 to P-4 in sequence, as shown in Table 3 where F_t is the estimated axial ultimate capacity and f_t the estimated static strength of the anchorage system. Static tensile tests were conducted again for the specimens that had undergone successfully the fatigue tests for determining the effect of fatigue loading on the anchoring capacity of adhesively bonded anchorage.

In order to monitor the real-time status and to develop a better understanding of the mechanism of fatigue damage in adhesively bonded anchorage systems, some temperature strain gauges were adhered to the surface of the CFRP tendon in the anchoring zone. The real-time temperature of the anchorage zone was monitored by a device of thermocouple thermometer (GM1312) during the course of fatigue loading.

Further, staged cyclic loading tests at frequencies 10 Hz (fatigue stress ratio is 0.76) and 12 Hz (fatigue stress ratio is 0.6) were performed on Specimens P-5, P-6 and P-7 to investigate the whole process and mechanism of the temperature rise in the anchorage system under fatigue loading. In these tests, the loading was terminated for 12 hours when the cycle counts reached the targeted count in order to ensure that the internal heat produced in the previous stages was dissipated completely. The next phase of the cyclic loading started thereafter. By doing this, the temperature rise recorded at each stage was restricted to the fatigue loading at the current stage, i.e., the temperature rise is independent of the heat accumulated in previous stages.

3. Experimental Results

During the static tests, the ultimate tensile capacity F_t for the specimens were measured and recorded in Table 2. Three kinds of failure modes were observed:

- Failure mode I: debonding failure at the interface between sleeve and bonding material;
- Failure mode II: pull-out of tendon from the bonding material;
- Failure mode III: tendon fracture.

During the fatigue loading, the relationship between the applied force and system slippage may be expressed as a continuous hysteresis curve. Table 4 lists some data extracted from the maximal system slippage for Specimens P-1 to P-6 under the maximum load of 39.6kN and four different stress amplitudes $\Delta\sigma$ =36 MPa, 96 MPa, 125 MPa and 156 MPa. The curves of system slippage versus cyclic load are shown in Fig. 4. And the failure modes of the anchorage systems under fatigue loading were photographed and shown in Fig. 5.

The responses of the assemblies of the anchorage systems were simultaneously recorded during the tests. The load-strain curves of the sleeve of Specimen P-1 before and after the fatigue test are shown in Fig. 6. The variation of the axial strain of the tendon at the middle of the anchoring zone of Specimen P-1 with respect to the monotonous tensile loading before and after the fatigue test is shown in Fig. 7. Figure 8 shows some typical curves of the system slippage under tensile loading before and after fatigue tests.

During the second batch of static tensile tests conducted on Specimens P-1 to P-4 which had undergone the fatigue tests, an abrupt failure occurred in Specimen P-2 due to the torsion produced by an improper operation while reloading, leading to no results for Specimen P-2. The residual ultimate tensile capacities for Specimens P-1, P-3 and P-4 were tested to be 67.1kN, 71.2kN and 81.5kN, respectively.

The temperature in the anchorage zone was monitored at both ends of specimens during the fatigue loading. It varies with respect to the loading frequency and cycle count. The temperature of the upper end was denoted by the number '1' and that of the lower end by the number '2'. Using this notation, for example, temperatures of the upper end anchorage and the lower end anchorage of Specimen P-1 loaded at 8 Hz are designated as P-1-8-1 and P-1-8-2, respectively; where P-1 represents the specimen number, the number '8' the loading frequency and the last number '1' or '2' stands for the upper or the lower end anchorage. Typical curves of the real-time temperature on the interface between the tendon and the bonding mortar in the anchorage zone are depicted in Fig. 9. The temperature-rise curves for Specimens P-5, P-6 and P-7 at different stages are shown in Fig. 10. Some damage modes in the bonding mortar and CFRP tendon under cyclic loading are shown in Fig. 11.

4. Analysis and Discussion

4.1 Static Properties of Anchorage System

It can be seen from the experimental results in Table 2 that there is a large variation (about 25%) in the static anchoring forces F_t and the mean bonding stress as well as the failure mode due to the nature of the material and manufacturing process. In addition, there is a large difference in the anchorage efficiency coefficient which is applied to evaluate the anchoring performance and calculated by [23]

$$\eta = \frac{F_{test}}{F_{design}} \tag{1}$$

where η is the anchorage efficiency coefficient, F_{test} the failure force of the anchorage system and F_{design} the ultimate load capacity of the CFRP tendon based on its tensile strength as guaranteed by the manufacturer.

Overall, the anchorage system with Adhesive II provides a higher capacity than its counterpart that uses Adhesive I. It can be concluded that Adhesive II is a better bonding material. The data from static tests indicate that the anchorages with the bonding length of 200mm have a higher anchoring efficiency than that with the bonding length of 180mm or 160mm for 8mm-diameter CFRP tendons. This manifests that the length of 200mm is still an effective length for such an anchorage

system. In addition, the capacities provided by anchorages with the inner inclination angles of 3° and 4° are close to each other and both of them are superior over the anchorage with 0° inclination. Thus, the anchorages grouted with Adhesive II, the length of 200mm and the inclination of 3° are verified to be optimal in anchoring performance. For such an anchorage design, the average ultimate capacity is 85.8kN with a coefficient of variation of 4.6%.

In fact, due to the influence of such factors as big scatter of materials, machining accuracy of anchorage assemblies and nonuniformity of the resin mortar, the tensile strength of anchorage system may be rather different from one another. In view of the insufficiency of the acquired statistical data, it is assumed that the distribution of tensile capacity of anchorages is normal with a variable coefficient of 4.6% for the above specimens. This results in an estimated ultimate tensile capacity of 78.2 kN with a reliability of 95% for such an adhesively bonded anchorage system.

4.2 System slippage during Fatigue Loading

The results depicted in Fig. 4 and Table 4 indicate that the slippage of Specimen P-1 increases with respect to the cyclic loading with a gradual decreasing growth rate until the cycle number exceeds 600,000. Thereafter, the anchorage system may be regarded as stable under fatigue loads. Although the slippage-load curves for Specimens P-2, P-3 and P-4 are somewhat different and the required cycle counts for the system stability under fatigue loading are different, all curves exhibit a similar trend of system slippage; an increasing slippage with respect to cycle counts and then the increase gradually come close to zero. Besides, the slippages of Specimens P-5 and P-6 increase with respect to cycle count in the first stages until the maximum slippage and thereafter the slippages become smaller, and finally get contained with a small variation range. This phenomenon implies that the anchorage system tends to be more stable after fatigue loading. This implies that a number of cyclic loading may be beneficial in improving the synergy of the different components (such as the sleeve, the bonding material and prestressed tendon) in the anchorage system.

It can also be seen from Fig. 4, that when the maximum fatigue load is 39.6 kN (50.6% of F_t) and the stress amplitude $\Delta\sigma$ < 10.6% of f_t, the increase of the stress amplitude may lead to a stable state of the system earlier under fatigue loading. By comparing the different specimens, we find that

- For Specimen P-1 where the stress amplitude is 2.3% of f_t, the slip stops after 600,000 cycles with a maximum slippage of 0.65mm, and the anchorage system becomes stable finally;
- For Specimen P-2 where the stress amplitude is enhanced to 6.1% of f_t, the system becomes stable after 200,000 cycles with a maximum slippage of 0.97 mm;
- For Specimen P-3, the stress amplitude of 8.1% of f_t makes the anchorage system stable before 200,000 cycles with a maximum slippage of 0.74 mm;
- However, the slippage may increase continuously under cyclic loading when the stress amplitude becomes relatively large. For example, for Specimen P-4 with a stress amplitude of 10.6% of f_t, the maximum system slippage is 2.52mm and the specimen is unstable before 600,000 cycles of loading;

- The variation of cycle counts needed for system stability and the maximum slippage of Specimens P-2, P-3 and P-4 from Specimen P-1 indicates that the stress amplitude influences the fatigue resistance of bonded anchorage systems significantly.

The above phenomena may be explained as follows. When the stress amplitude and the level of fatigue stress are small, the increase in stress amplitude leads to a larger relative displacement between the tendon (and bonding material together) and the sleeve in the initial stage of cyclic loading. Most part of the relative displacement is not recoverable. As a result, the anchorage assemblies become closer to one another in the geometric cone and thus, a greater normal stress as well as a greater friction force are generated on the tendon in the anchorage area. This helps to improve the anchorage tensile capacity. With the resistance provided by the increased friction force, the growth rate of the system displacement decreases gradually until the anchorage system becomes stable. However, when the stress amplitude or the level of fatigue stress is large enough to exceed their threshold values, the original micro-cracks in the anchorage assemblies and the interfacial debonding will develop and the damage worsen until failure of the anchorage system. During this period, the system slippage increases continuously with respect to the cycle number.

4.3 Effect of Fatigue Loading on Properties of Anchorage System

During the tests, fatigue damage was caused by the repeated superficial wear, as well as by the development of cracks and debonding, resulting in the loss of bonding force and triggering local failure of the anchorage system. Owing to the higher fatigue amplitudes exerted on Specimens P-3 and P-4, fatigue damage appeared not only at the interface between the tendon and bonding material, but also in the bonding mortar and the tendon; resulting in either the sliding failure of anchorage system (see Fig. 5a) or the final fracture of tendon or bonding mortar (see Fig. 5b). Sometimes anchorages failed by both sliding failure and tendon fracture.

The axial strain of sleeve depicted in Fig. 6 appropriately linearly grows with respect to the tensile load before and after the fatigue test. However, the axial strain-load curve obtained after the fatigue test has a lower slope. Considering that there was no damage in the steel sleeve, the increased strain in the steel sleeve indicates a slight improvement of the steel sleeve in resisting the axial load after the fatigue test. The sleeve's circumferential strain-load curves before and after fatigue test do not vary much from each other. But its linear feature after fatigue test gets more distinct as the axial loading increases monotonically. This small difference between the linear characteristic of the curves suggests a stress redistribution due to slipping of micro particles near the interface between the tendon and bonding mortar since the circumferential stress of the sleeve is related to the transverse synergy of the anchorage components [16]. This also indicates a better synergy of the anchorage components after fatigue loading.

Based on the comparison of the axial strains of the CFRP tendon before and after fatigue tests shown in Fig. 7, it can be seen that the tendon's load-strain curves from the postfatigue monotonic tensile tests are remarkably different from the original ones. The latter are strictly linear when the static load is below 30kN while nonlinear

characteristics of the load-strain curves were observed after fatigue test. When the entire tensile load is less than 50kN, the strain of the tendon rises slowly. Once the load is beyond 50kN, the strain rises rapidly with a sharply lower slope. This variation indicates that when the entire tensile load is lower than 50kN, the force taken by the CFRP tendon is much smaller than that before the fatigue test, while a bigger part of the entire load is borne by the adhesive and the sleeve of anchorage system. The anchorage system bears the total load through the synergistic action of the tendon, the bonding material and sleeve. It is thus clear that the synergistic action of the anchorage system is improved by the cyclic loading. However, the slope of the curve decreases when the tension is close to the failure load. The possible mechanism for this observation is the occurrence of local damage which becomes serious (i) in the bonding mortar, (ii) in the tendon and (iii) on the interface between the bonding mortar and the tendon with the propagation of micro-cracks in the anchorage system. The damage is accompanied by an increase in the surface area for debonding and by the degradation of mechanical properties of bonding mortar as well as the interfacial properties between the bonding mortar and the tendon. Consequently, the load undertaken by the bonding mortar becomes smaller and a large portion of the entire load is redistributed to the CFRP tendon because it offers a strong resistance to fatigue. Consequently, the ultimate tensile capacity of the specimen after fatigue loading becomes less than the initial ultimate tensile strain.

In fact, the residual capacities of Specimens P-1, P-3 and P-4 decreased by 5.3%, 17.9% and 8.7%, respectively, compared to their initial tensile capacities; i.e. an average decrease of 10.6%. Among Specimens P-1, P-3 and P-4, Specimen P-1 had the lowest stress amplitude and the smallest slippage in its anchorage zone. Therefore, there is less wear at the interface between the tendon and resin mortar. This explains why the tensile capacity of Specimen P-1 exhibited the smallest decrease. In sum, all these results indicate that the anchorage system with a bonding length of 200mm, an inclination of 3° and Adhesive II is able to maintain the tensile capacity rather well during cyclic loading. This finding demonstrates that the anchorage system performs very well against fatigue loading and so this anchorage system is reasonably acceptable for 8mm-diameter CFRP tendons.

From Fig. 8, the slippage-load curves of Specimens J-1, J-2, J-6 and J-8 (before fatigue test) are basically linear at the early stage, but the slippage increases abruptly and irregularly when the tensile load is close to the ultimate tensile capacity of the anchorage system. In contrast, the slippage curves of Specimens P-1, P-2 and P-3 (after fatigue test) are more regular at the early stage, and their knee points (sudden change in slope) appear in advance. These curves are almost linear with a small slippage until the applied stresses reach their maximum fatigue stresses. After that, the specimens begin to slip sharply until the failure of the anchorage system; featuring a slightly lower average ultimate tensile strength. This illustrates that the slippage resistance of the bonded anchoring system does not drop after fatigue loading when the static load is below the maximum fatigue load. However, the anchoring performance may decline when the service load exceeds the maximum fatigue load.

Therefore, the cyclic loading in a low-stress state improves the synergistic action of the anchorage components and the stability of the anchorage system. This finding is consistent with the earlier researchers' [34] conclusions. However, the cyclic loading with a high-stress amplitude may reduce the axial stiffness of the anchoring system; thereby leading to a bigger fatigue damage or even an abrupt failure of the anchoring system.

Below, the technical explanation for the behavior of the anchorage system under fatigue loading is given. Under cyclic axial loading, stress concentrations are developed at the interface between the CFRP tendon and the bonding mortar, or at the interface between the bonding material and sleeve, as well as in the resin mortar where micro bubbles and microcracks exist. Consequently, Mode-II cracks (or micro-slipping cracks) may appear prematurely in these aforementioned regions under fatigue loads. These microcracks may continue to develop under repeated tensile loads as well as shearing and contact stresses leading to a partial debonding failure. Consequently, the system slippage increases or even the anchorage system fails. Figure 11(a) shows the partial debonding failure in the adhesive region that is close to the interface between the tendon and resin mortar, and Fig. 11(b) shows a macrocrack formed on the surface of the tendon where we discover an amazing counteracting effect from the notches on the tendon surface in reducing the crack width.

Cyclic longitudinal movements of the tendon in the resin mortar will produce and accelerate the interfacial debonding. The debonding regions wear down in the continuing cyclic loading. The fretting damage changes the coefficient of friction along the debonding surfaces from a slight increase at the beginning stage to degradation in the long term. Consequently, damage or even an irrecoverable slippage is produced in the anchorage system. However, as mentioned earlier, the anchorage system can become more stable after cyclic loading unless the stress amplitude is too high to lead to the failure of the anchorage system. This paradoxical stability may be explained by the extension of the debonding surface caused by the development of micro-cracks, which brings out the following interesting effects:

- The local microstructure of the interface may slide or be broken under cyclic loading, resulting in the accumulation of debris along the interface and the increase of the coefficient of friction. This enhances the sliding-resistance of the anchorage system. Although it is difficult to measure the damage in the anchorage system because of the uneven distribution of bonding stress in the anchorage zone, the debris accumulation of other epoxy-based composite materials has been observed in fatigue tests [35, 36].
- As the fatigue resistance of the resin-based materials is far lower than that of the fibers, more microcracks appear and develop in the bonding mortar. In addition, partial debonding failure occur more frequently at the interface between the fiber and the resin mortar. These two factors relieve the stress concentration in the anchorage system and thereby enhancing the anchoring capacity. Support for this mechanism was partly obtained from the multiply failure modes appeared in the anchorage system after fatigue tests instead of the appearance of one main failure mode.
- A repeated loading within an appropriate level can adjust the possible bias of

the system by promoting a more orderly arrangement of the micro-structures of the bonding material along the principal axis and thus improving the uniformity of stress distribution. A higher strength and stiffness could be obtained for the system in the initial loading stage, which can be confirmed partly by a more uniform change of the circumferential strain of the sleeve after cyclic axial tensile loading as shown in Fig. 6.

On the other hand, the application of a very large stress will seriously reduce the ultimate anchoring capacity of the system due to easier formation of macro-cracks and the debonding surface throughout the interface that will lead to either slip failure or fracture failure of bonding material or tendon.

4.4 Effect of Loading Frequency on Temperature Rise in Anchorage Area

As shown in Fig. 9, the temperature rise increases as the rise of loading frequency during the cyclic loading. The temperatures at the two anchorage ends increased very slowly when the loading frequency was 8Hz and reached their maximum values at about 430,000 cycles and 450,000 cycles, respectively. Thereafter the temperatures remained almost constant. The average maximum temperature rise was 1.2°C during the whole fatigue loading process. The same tendency was obtained when the cyclic loading frequency was 10 Hz. The temperature also increased slowly at the starting phase until both maximum temperatures were reached at 450,000 and 430,000 cycles, with the respective temperature rise of 1.4°C and 1.0°C. After that, the temperature fluctuated slightly about the maximum temperature; indicating a stable state of the system under fatigue loading. However, when the loading frequency was increased to 12 Hz, the temperatures in two anchorage ends went up remarkably at the starting phase and was accompanied by a large growth rate until the maximum temperatures were reached at 187,000 and 65,000 cycles. The maximum temperature rise was 5.9°C for the upper anchorage end and 4.0°C for the lower anchorage end. After reaching the maximum temperature, the temperature decreased gradually with respect to the cycle count. Finally, the temperatures at both anchorage ends were stable after 490,000 cycles.

Based on the results from the staged fatigue tests shown in Fig.10, the following conclusions may be drawn:

- Generally, a higher loading frequency with the same stress ratio results in a higher temperature rise, which is consistent with the phenomenon shown in Fig. 9. Therefore, the influence of loading frequency on the temperature rise is significant, especially when the loading frequency is more than 10Hz.
- Temperature rise varies pronouncedly in different loading stages. Under the two loading conditions in this case, the temperature rises fairly slowly in the first two stages despite of the big scatter. In the third loading stage, the temperature increases sharply and reaches its maximum value rapidly. It is worth mentioning that the third stage of the Specimen P-5 corresponds to the cumulative cycles from 400,000 to 600,000, with a maximum temperature rise of 3.2°C. The third stage of Specimens P-6 and P-7 corresponds to the cumulative cyclic count from 350,000 to 600,000 with the maximum temperature rise of 3.1°C and 3.5°C, respectively. In the fourth and fifth cyclic loading stages, the temperature rise of

Specimens P-6 and P-7 changes slightly. Since the specimens were reloaded only after the dissipation of inner heating cumulated in the previous stages, it can be concluded that the inner friction heating is produced unevenly during cyclic loading. The intensive phase of inner friction heat is from the early-to-mid stage. The production of the inner friction heat at the late stage nearly balances the heat dissipation of the anchorage system.

- It is worth noting that the total temperature rise in staged tests with the same stress ratio (Specimens P-6 and P-7 in Fig. 10) is higher than the counterpart in the continuous fatigue loading tests (Specimen P-4 in Fig. 9). The main reason for this is that the rate of heat dissipation for Specimen P-4 is faster than that for Specimens P-6 and P-7 because of the much higher temperature peak in the continuous loading tests. This observation embodies the effect of balance of heat generation and heat dissipation on the temperature rise.

As presented in the continuous loading tests, the temperature variation in the anchorage system was affected by the loading frequency and stress amplitude. When the loading frequency is high, the specimen does not have sufficient time to lower the stress concentration or to redistribute the stress via increasing microcracks and local debonding damage. Moreover, the system has less time to dissipate the generated heat. Thus, the strength and stiffness of the specimen are hardly improved at the initial stage.

With regard to the sources of the inner friction heat in the adhesively bonded anchorage system for resin-based CFRP tendons during cyclic loading, there are three ways in which the friction heat is generated:

- the relative slippage between the fiber and the matrix and between the CFRP tendon and bonding mortar;
- friction between the debonding surfaces; and
- friction between fractured fibres under high stress or high stress amplitude that breaks the fibers.

Therefore, a higher loading frequency leads to the production of more friction heat in the anchorage area for a given time period. This in turn accelerates the development of microcracks and system slippage as well as the degradation of the mechanical properties of the composite materials due to the sensitivity of the applied resin in the bonding mortar and CFRP tendon to heat. In addition, a high stress amplitude plays the same role during the fatigue loading because more serious debonding and cracking often occur in the anchorage zone while keeping the other loading conditions constant. Consequently, specimens subjected to cyclic loading with a high frequency or a high stress amplitude (such as Specimen P-4) suffer more damage and experience higher friction heat releases. The temperature rise is also caused by the unbalanced status between the generated friction heat (which is related with loading conditions, such as frequency and stress amplitude) and the heat dissipation capacity (due to conduction and convection) in the same phase. However, one may regard the variation of the temperature rise as an indicator on the extent of microstructural damage based on the following considerations:

- The temperature is measured in real time on the interface between the tendon and the bonding mortar and thus, the temperature variation is highly dependent on the real-time interfacial friction heat.
- As both tendon and bonding mortar in the anchorage area are sealed by the sleeve, the heat dissipation by convection cannot happen; thereby decreasing the inner heat dissipation capacity of the anchorage system.
- The heat conduction capacity is highly related to the difference in temperatures between the outer surface and the friction surface. In the early stage of loading, the heat dissipation capacity is weak due to the small temperature difference. Consequently, the temperature rise in the early stage mainly depends on the interfacial friction heat. Thus, the temperature rise could indeed be used as an indicator for the extent of structural damage.
- In the mid-stage of loading, the heat dissipation capacity increases with respect to the temperature difference. Thus, a unit temperature rise in this mid-stage implies that more friction heat is generated in the structure than that in the early stage. In this respect, the increase in temperature rise indicates a fast development of structural damage. Moreover, a higher rate of temperature rise is an indicator of a more serious damage.
- When the heat generation is equal to the heat dissipation, there is no temperature rise. This is the moment when the heat dissipation reaches its maximum and the development of structural damage slows down until the anchorage system reaches a stable state.

The above posit may be validated by comparing the temperature variation and the system slippage. Figure 12 presents a comparison of the temperature rise and the system slippage of Specimen P-4 under cyclic loading with the loading frequency of 12Hz. The curves may be divided into three phases：

- Phase I: The maximum growth rate for the system slippage appears. Also the temperature increases rapidly to the maximum value.
- Phase II: System slippage continues to increase but with a lower growth rate (which means the generation rate of the friction heat slows down). Simultaneously the temperature keeps stable or even declines (which means the rate of heat dissipation is increasing continuously and may even begin to exceed the generation rate of the friction heat).
- Phase III: Both the temperature and anchorage system slippage are basically stable (which means that there is a rebalance between heat generation and heat dissipation and no new damage occurs in the anchorage system).

The comparison of the results in Fig. 12 indicates that the temperature variation is related to the sliding and internal damage of the anchoring system although it is not completely synchronous with the system slippage due to the effect of heat dissipation. This supports the conclusion that the loading frequency and fatigue stress amplitude have similar effects on the microstructural damage and on the friction heat. The trend in the variation of the inner temperature reflects the extent of the microstructural damage in the anchorage zone to some extent.

It is worth noting that for specimens subjected to a high-frequency high-stress amplitude loading, the friction heat at the interface may result in a large growth rate of interfacial temperature. The difference between the internal temperature and the external temperature becomes larger which leads to an increasing rate of heat dissipation. When the rate of heat transfer begins to exceed that of heat production, the interface temperature may decrease with a lower transfer rate. This explains why there is a descending phase in the temperature curve for Specimen P-4. Finally, the interfacial temperature becomes stable when the heat conduction balances the heat production.

5 Conclusions

Experimental investigations were performed on adhesively bonded anchorage systems for CFRP tendons under cyclic axial tension-tension loading. The following key conclusions may be drawn:

- The anchorage system with a bonding length of 200mm, an inclination of 3° and Adhesive II was recommended for 8mm-diameter CFRP tendon due to its excellent static anchoring capacity, as well as good fatigue resistance.
- Stress amplitude affects the system slippage of a bonded anchorage system. The anchorage system tends to be stable under fatigue loading provided that the stress amplitude is fairly low. A measured amount of stress amplitude improves the performance of the anchoring system by stabilizing the system earlier.
- The axial tension-tension loading will reduce the ultimate anchoring capacity. The reduction primarily depends on the stress amplitude. If the stress amplitude and the maximum fatigue stress are fairly low, the anchorage system can maintain the tensile capacity well under repeated loading.
- The temperature rise of the anchorage is strongly related to the loading frequency and the stress amplitude. On the condition that the stress amplitude is below the fatigue threshold, the temperature rise is not obvious when the loading frequency is low (say 8Hz or 10Hz). However, the variation of temperature will become pronounced when the loading frequency is raised to 12 Hz. Moreover, friction heating occurs mainly at the early- and mid-stage of cyclic loading. There is little change in temperature at the latter stage of cyclic loading.
- A temperature rise is associated with irrecoverable damage in the anchoring system caused by fatigue loading. The concentration of friction heating is quite different in various phases of the loading process. Further studies should be performed to establish the quantitative relationship between the temperature rise and the damage in the anchoring system, as well as the loading conditons. The studies should include experimental investigations and the application of mesoscopic mechanics and three-dimensional heat conduction theory.

Acknowledgements

The authors gratefully acknowledge the financial supports from the National Natural Science Foundation of China (No. 51508235 and No. 51478209), Jiangsu Province

Science Foundation for Youths (No. BK20140553) and Natural Science Foundation of Jiangsu Education Department for Colleges and Universities (No. 17KJD580002). And the authors appreciate the reviewers for their valuable comments for the paper.

References

[1] Tsujii M, Kanno R. Advances in steel structures and steel materials in japan, *Nippon Steel and Sumitomo Metal Technical Report* 2016; *113*: 3-12.

[2] <https://corrosion-doctors.org/Bridges/Introduction.htm>

[3] Haghani R, Al-Emrani M, Heshmati M. Fatigue-prone details in steel bridges. *Buildings* 2012; 2: 456-476.

[4] Ghafoori E, Asghari M. Dynamic analysis of laminated composite plates traversed by a moving mass based on a first-order theory. *Composite Structures* 2010; 92: 1865–1876.

[5] Liu Y, Zwingmann B, Schlaich M. Carbon fiber reinforced polymer for cable structures—a review. *Polymer* 2015; 7(10): 2078-2099.

[6] Hollaway L C. A review of the present and future utilisation of FRP composites in the civil infrastructure with reference to their important in-service properties; *Construction and Building Materials* 2010; 24(12): 2419-2455.

[7] Xie G, Yin, J, Liu R, Chen B, Cai D. Experimental and numerical investigation on the static and dynamic behaviors of cable-stayed bridges with CFRP cables. *Composite Part B* 2017; 111: 235-242.

[8] Yang Y, Wang X, Wu Z. Experimental study of vibration characteristics of FRP cables for long-span cable-stayed bridges. *Journal of Bridge Engineering* 2015; 20(4): 04014074.

[9] Cai H, Aref A J. On the design and optimization of hybrid carbon fiber reinforced polymer-steel cable system for cable-stayed bridges. *Composite Part B* 2015; 68: 146-152.

[10] Lee H, Lee W, Jung WT, Chung W. Bond characteristics of near-surface-mounted anchorage for prestressing. *Construction and Building Materials* 2017; 148: 748-756.

[11] Cai D, Yin J, Liu R. Experimental and analytical investigation into the stress performance of composite anchors for CFRP tendons. *Composites Part B* 2015; 79: 530-534.

[12] Campbell T I, Shrive N G, Soudki KA, Al-Mayah A, Keatley JP, Reda MM. Design and evaluation of a wedge-type anchor for fibre reinforced polymer tendons. *Canadian Journal of Civil Engineering* 2000; 27: 985-992.

[13] Puigvert F, Crocombe AD, Gil L. Static analysis of adhesively bonded anchorages for CFRP tendons. *Construction and Building Materials* 2014; 61: 206-215.

[14] Li F, Zhao Q, Chen H, Wang J, Duan J. Prediction of tensile capacity based on cohesive zone model of bond anchorage for fiber-reinforce dpolymer tendon. *Composite Structures* 2010; 92: 2400–2405.

[15] Feng P, Zhang P, Meng X, Ye L. Mechanical analysis of stress distribution in a carbon fiber-reinforced polymer rod bonding anchor. *Polymers*, 2014, 6(4): 1129-1143.

[16] Xie G, Liu R, Chen Be, Li M, Shi T. Synergistic effect of a new wedge-bond-type anchor for CFRP tendons. *Journal of Central South University* 2015; 22(6): 2260−2266.

[17] Fang Z, Zhang K, Tu B. Experimental investigation of a bond-type anchorage system for multiple FRP tendons. *Engineering Structures* 2013; 57: 364–373.

[18] Meier, U. Extending the life of cables by the use of carbon fibres. *Proceedings of the IABSE Symposium*. San Francisco, Calif., 1995; 1235-1240.

[19] Schmidt J W, Bennitz A, Täljsten B, Goltermann P, Pedersen H. Mechanical anchorage of FRP tendons – A literature review. *Construction and Building Materials* 2014; 32: 110–121.

[20] Meier, U, Meier H, Kim, P. Anchorage Device for High-Performance Fiber Composite Cables. U.S. Patent US 5,713,169 A, 3 February 1996.

[21] Alsheraida O S, El-Gama S. performance of modified wedge anchorage system for pre-stressed FRP bars. *World academy of science, Engineering and Technology International Journal of Civil and Environmental Engineering* 2015; 9(10):1285-1289.

[22] Elrefai A, Jeffrey West SJ, Soudki K. Performance of CFRP tendon–anchor assembly under fatigue loading. *Composite Structures*, 2007; 80(3): 352–360.

[23] Han Q, Wang L, Xu J. Test and numerical simulation of large angle wedge type of anchorage using transverse enhanced CFRP tendons for beam string structure. *Construction and Building Materials* 2017; 144: 225-237.

[24] Ferrier E, Bigaud D, Clement JC, Hamelin P. fatigue-loading effect on RC beams strengthened with externally bonded FRP. *Construction and Building Materials* 2011; 25: 539-546.

[25] Charalambidi B, Rousakis T, Karabinis A. Fatigue behavior of large-scale reinforced concrete beams strengthened in flexure with fiber-reinforced polymer laminates. *Journal of Composites for Construction* 2016; 20(5): 04016035-1 – 04016035-10.

[26] Charalambidi B, Rousakis T, Karabinis A. Analysis of the fatigue behavior of reinforced concrete beams strengthened in flexure with fiber reinforced polymer laminates, *Composites Part B* 2016; 96: 69-78.

[27] Wang YC, Lee MG, and Chen BC. Experimental study of frp-strengthened RC bridge girders subjected to fatigue loading. *Composite Structures*, 2007; 81: 491–498.

[28] Ghafoori E, Motavalli M, Zhao X, Nussbaumer A, Fontana M. Fatigue design criteria for strengthening metallic beams with bonded CFRP plates. *Engineering Structrues* 2015; 101: 542-557.

[29] Martinelli E, Caggiano A. A unified theoretical model for the monotonic and cyclic response of FRP strips glued to concrete. *Polymers* 2014; 6: 370-381.

[30] Martinelli E, Zhou H, Fernando D. Cyclic response of frp-to-concrete adhesive joints: effect of the shape of bond-slip model. *SMAR-Fourth Conference on Smart Monitoring, Assessment and Rehabilitation of Civil Structures* 2017.

[31] Puigvert F, Crocombe AD, Gil L. Fatigue and Creep Analyses of Adhesively Bonded Anchorages for CFRP Tendons. *International Journal of Adhesion & Adhesives* 2014; 54(5): 143-154.

[32] Zhege P, Ding Y, Hou W, Qiang S. Optimization Design and Fatigue Test of New CFRP Tendon Anchor Assembly. *Journal of Zhejiang University* (Engineering Science) 2014; 48(10): 1822-1827.

[33] *Technical Specification for Application of Anchorage, Grip and Coupler for Prestressing Tendons* (J1006-2010), China, 2010.

[34] Fang Z, Gong C, Yang J, Sun Z. Fatigue behavior of bond-type anchorage with CFRP tendon. *Journal of Highway and Transportation Research and Development*, 2012, 29(7): 58-63.

[35] Saunders DS, Galea SC, Deirmendjian GK. The development of fatigue damage around fastener holes in thick graphite/epoxy composite laminates. Composites 1993; 24: 309-323.

[36] Ritchie RO. Mechanisms of fatigue crack propagation in metals, ceramics and composites: role of crack tip shielding. Materials Science and Engineering 1988; A103:15-28.

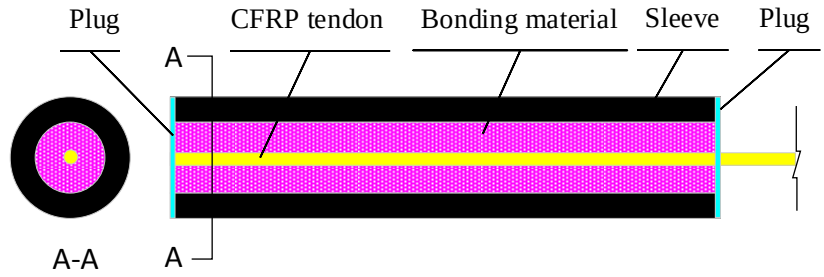

(a) Adhesively bonded anchorage system

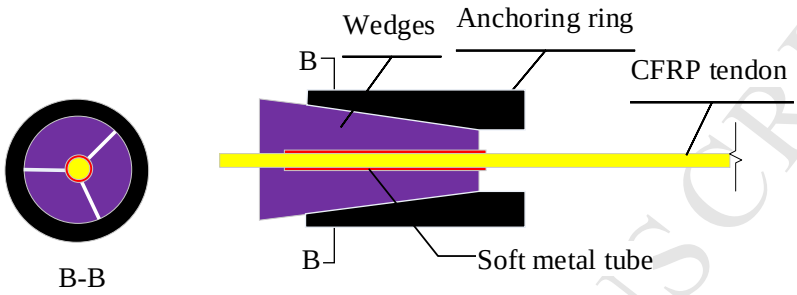

(b) Mechanical clamping anchorage system

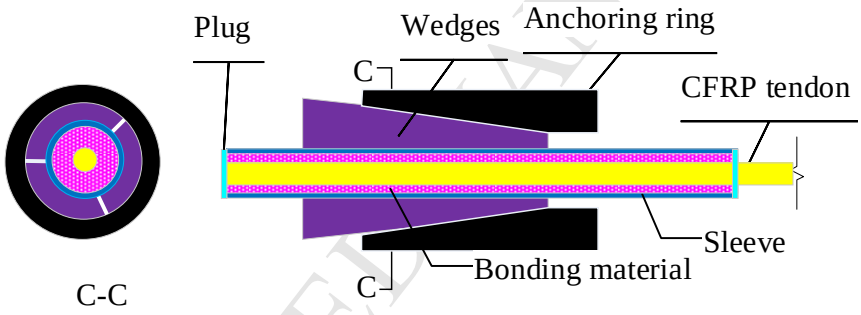

(c) Composite anchorage system

Fig.1 Three types of anchorage systems for CFRP tendon

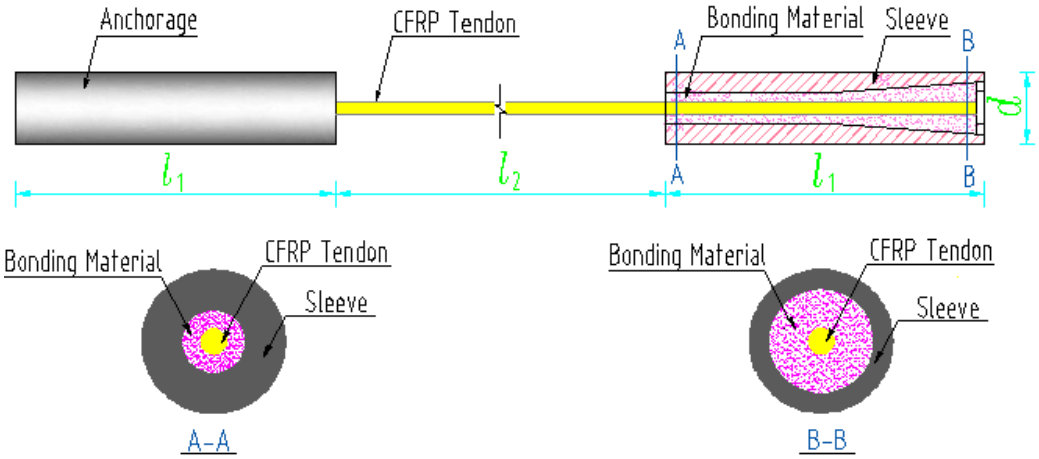

Fig. 2 Adhesively bonded anchorage for CFRP tendons

(a) MTS 809

(b) PA-500 fatigue tester

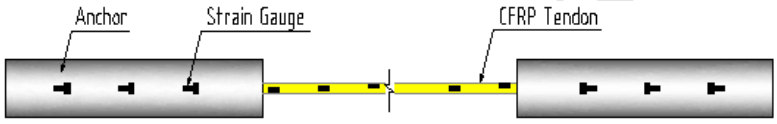

(c) Layout of strain gauges on anchorage system

Fig. 3 Experimental setup of static tests

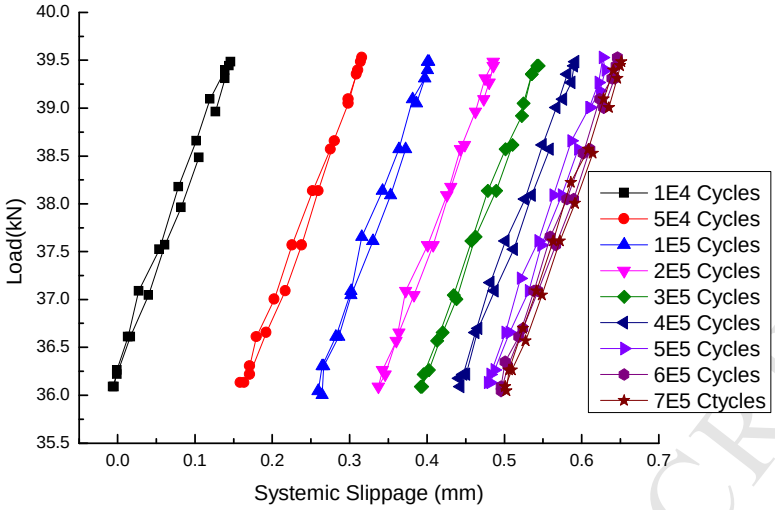

(a) Specimen P-1

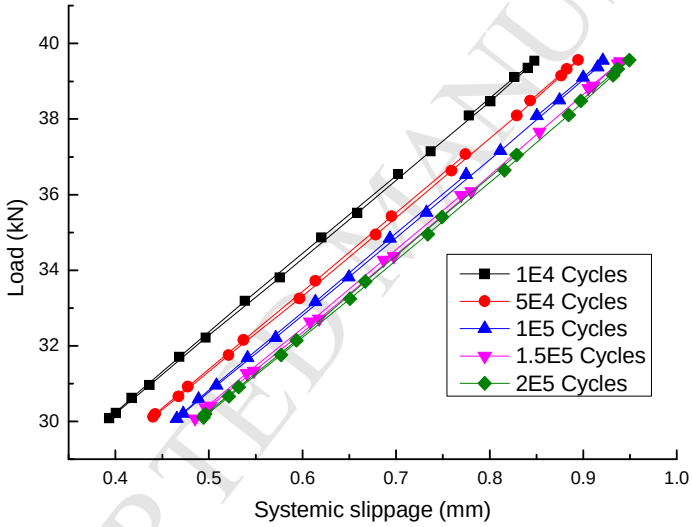

(b) Specimen P-2

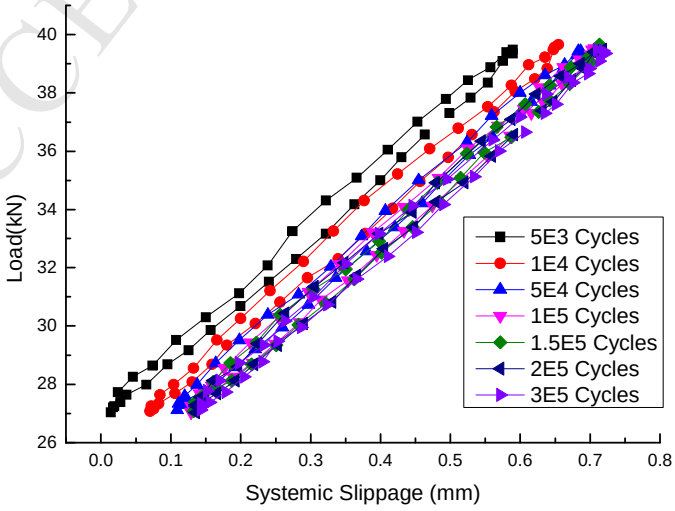

(c) Specimen P-3

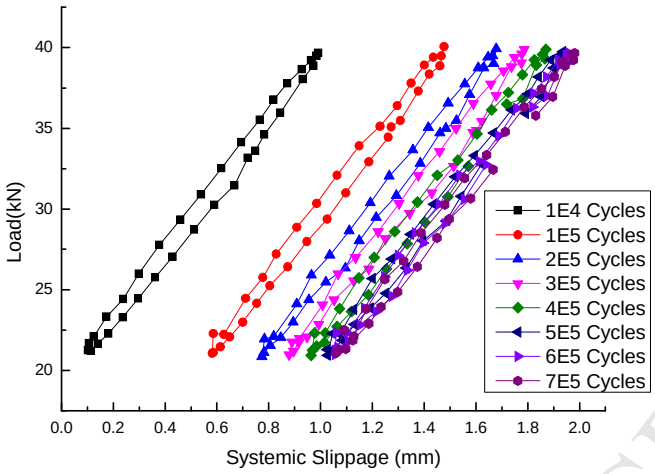

(d) Specimen P-4

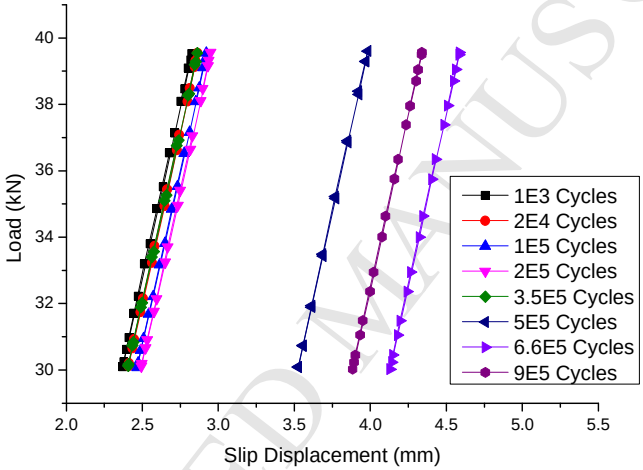

(e) Specimen P-5

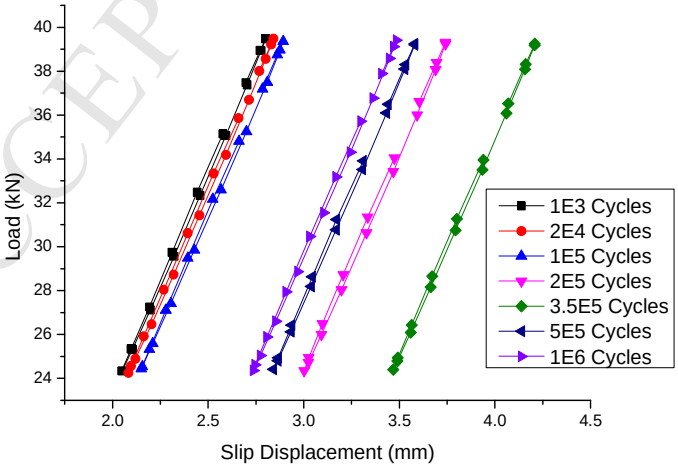

(f) Specimen P-6

Fig. 4 Slippage versus load curves with maximum load of 39.6kN

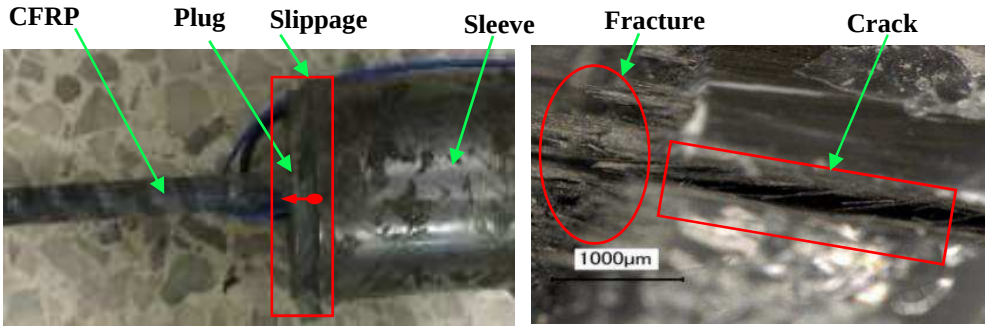

(a) Slippage (b) Fracture of tendons

Fig. 5 Failure of anchorage system under fatigue tests

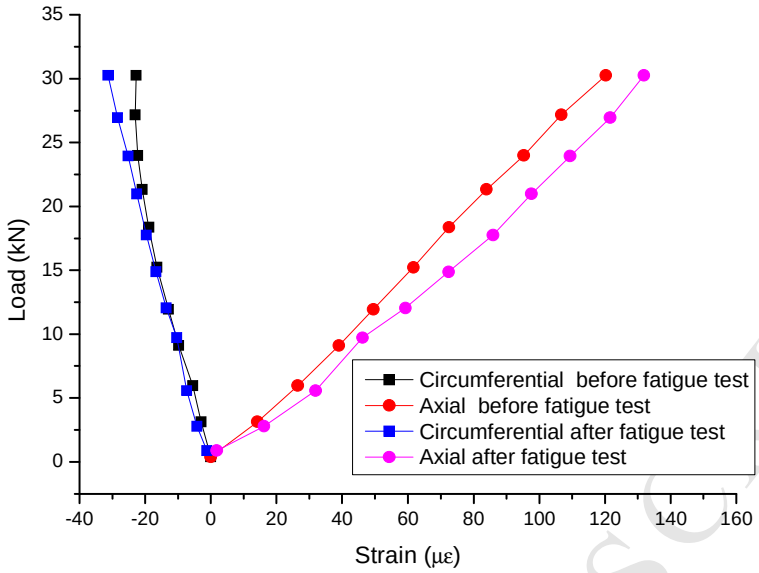

Fig. 6 Load-strain curve of steel sleeve in static tensile test before and after fatigue

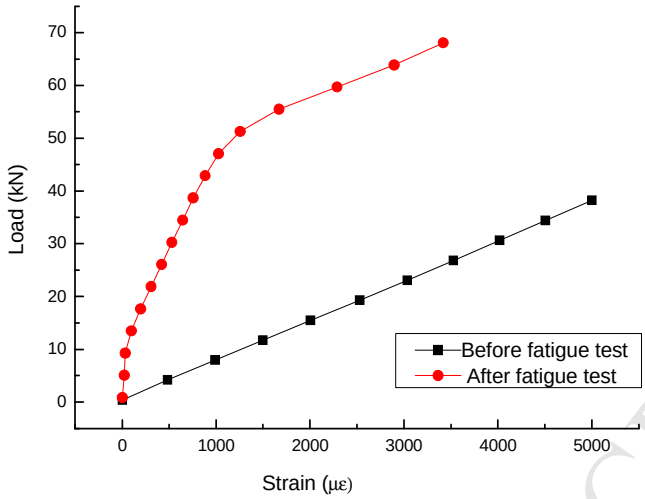

Fig.7 Axial strain of CFRP tendons before and after fatigue tests

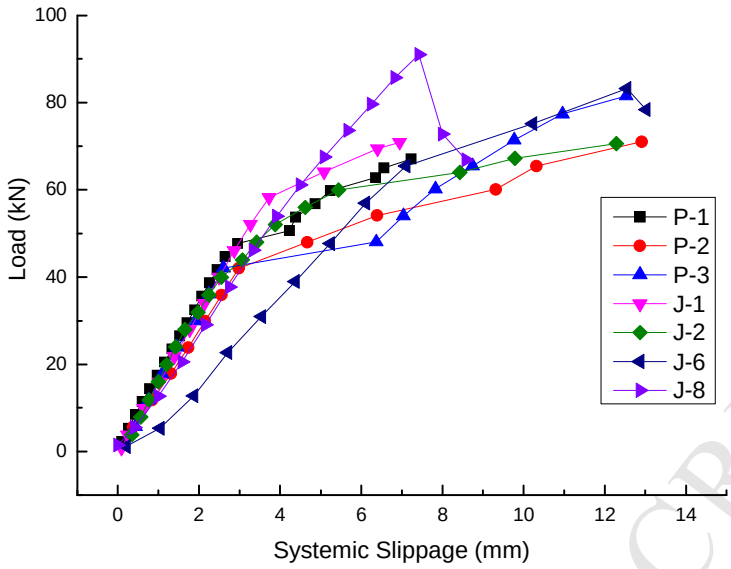

Fig. 8 Load-slippage curves during static test before and after fatigue tests

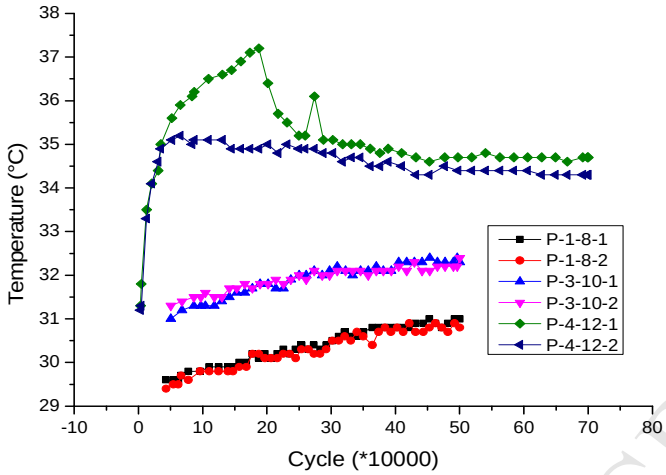

Fig. 9 Temperature variations in anchorage zones for different cyclic loading frequencies

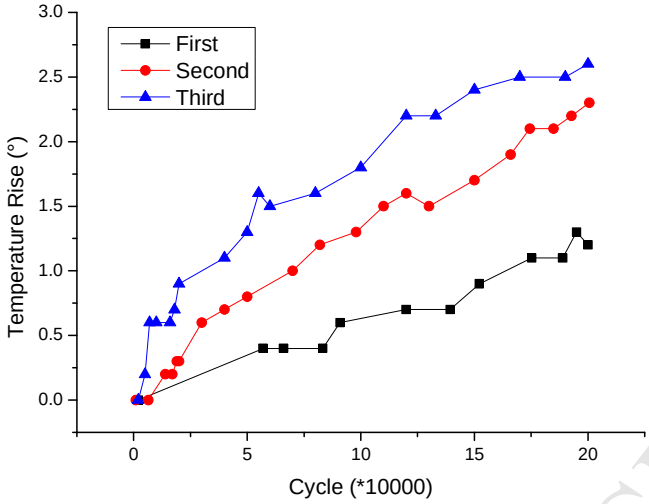

(a) P-5，frequency *f*=10Hz, stress ratio=0.76

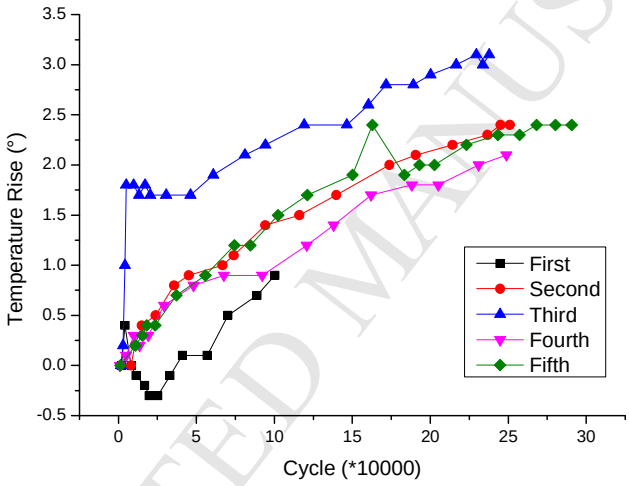

(b) P-6，frequency *f* =12Hz, stress ratio=0.6

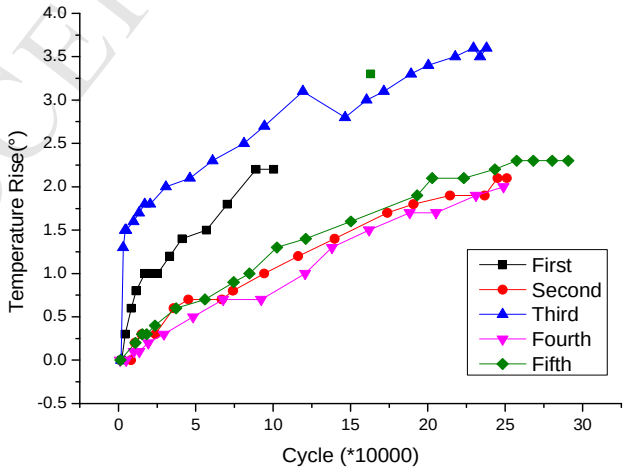

(c) P-7, frequency *f* =12Hz, stress ratio=0.6

Fig.10 Temperature curves in anchorage zone at different frequencies

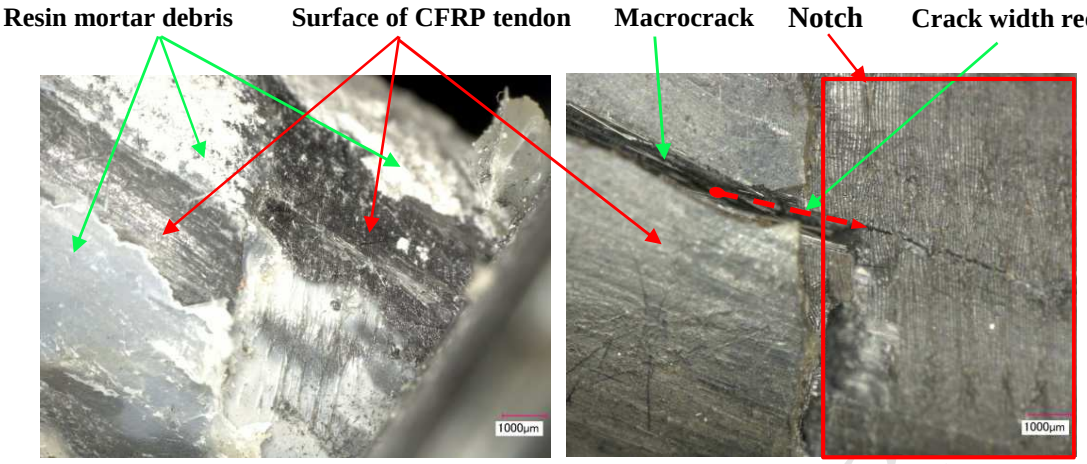

(a) Debonding in adhesive close to interface (b) Cracks in CFRP tendons

Fig. 11 Damage in anchorage system

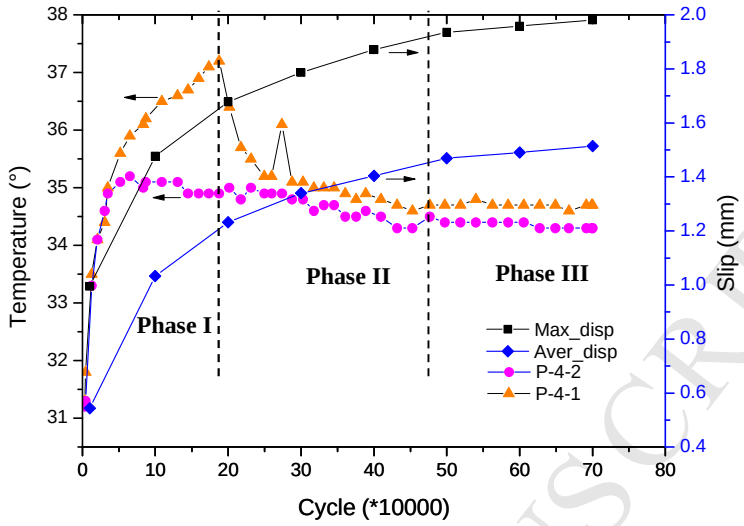

Fig.12 Temperature and system slippage under cyclic loading

Table 1 Physical and mechanical properties of CFRP tendons

Surface	Diameter of tendon (mm)	Longitudinal UTS (MPa)	Longitudinal modulus (GPa)	Longitudinal Poisson's ratio	Transverse modulus (GPa)	Transverse Poisson's ratio
Depressed	8	1800	147	0.27	10.3	0.02

Table 2 Structural parameters and results of specimens in static tests

Specimen number	l_1 (mm)	Inclination (°)	Adhesive	F_t (kN)	Bonding stress (MPa)	η (%)	Failure mode
J-1	200	3	Adhesive Ⅰ	70.9	14.11	78.4	II
J-2	200	3	Adhesive Ⅰ	70.6	14.05	78.1	I
J-3	200	3	Adhesive Ⅱ	86.7	17.26	95.9	II
J-4	200	3	Adhesive Ⅱ	89.3	17.77	98.7	II
J-5	200	3	Adhesive Ⅱ	85.6	17.04	94.7	II
J-6	200	3	Adhesive Ⅱ	81.8	16.28	90.5	II
J-7	200	3	Adhesive Ⅱ	79.4	15.80	87.8	II
J-8	200	3	Adhesive Ⅱ	91.8	18.27	101.5	III
J-9	200	4	Adhesive Ⅱ	90.1	17.93	99.6	III
J-10	200	0	Adhesive Ⅱ	75.4	15.00	83.4	II
J-11	180	3	Adhesive Ⅱ	82.1	18.16	90.7	II
J-12	180	0	Adhesive Ⅱ	68.5	15.15	75.8	II
J-13	160	3	Adhesive Ⅱ	78.5	19.53	86.8	II

Table 3 Loading conditions for fatigue tests

Specimen number	Maximum Load F_{max} (kN)	Minimum Load F_{min} (kN)	Stress Amplitude Δσ (MPa)	Frequency f (Hz)	Testing device
P-1	39.6（50.6%F_t）	36（46.0% F_t）	36(2.3% f_t)	8	PA-500
P-2	39.6（50.6% F_t）	30（38.3% F_t）	96(6.1% f_t)	10	PA-500
P-3	39.6（50.6% F_t）	27（34.5% F_t）	125(8.1% f_t)	10	PA-500
P-4	39.6（50.6% F_t）	24（30.7% F_t）	156(10.6% f_t)	12	PA-500
P-5	39.6（50.6% F_t）	30（38.3% F_t）	96(6.1% f_t)	10	MTS-809
P-6	39.6（50.6% F_t）	24（30.7% F_t）	156(10.6% f_t)	12	MTS-809
P-7	39.6（50.6% F_t）	24（30.7% F_t）	156(10.6% f_t)	12	MTS-809

Table 4 Maximal system slippage during fatigue loading (unit: mm)

Cycles	10k	50k	100k	200k	300k	400k	500k	600k	700k
P-1	0.148	0.314	0.406	0.489	0.542	0.592	0.631	0.645	0.651
P-2	0.848	0.895	0.921	0.949	—	—	—	—	—
P-3	0.655	0.686	0.706	0.718	0.722	—	—	—	—
P-4	0.99	1.271	1.477	1.679	1.787	1.870	1.935	1.958	1.976
P-5	2.848	2.895	2.921	2.949	2.850	2.867	3.982	4.423	4.542
P-6	2.824	2.867	2.892	3.741	4.108	4.015	3.580	3.484	—